

# Application of Ground Penetrating Radar in Glaciology and Permafrost Prospecting



By Stephan Gruber and Florian Ludwig, 12/1996

This document has been written as a Study Paper for the Arctic Studies Programme at the Arctic Centre, Rovaniemi, Finland, under the Supervision of Dr. John Moore.

# Table of Contents

<b>Abstract .....</b>	<b>3</b>
<b>Introduction .....</b>	<b>3</b>
<b>1. Understanding radar .....</b>	<b>4</b>
1.1. Electromagnetic radiation .....	4
1.2. Basic physics of radar .....	6
1.3. Principles of GPR applications .....	7
<b>2. GPR data interpretation .....</b>	<b>9</b>
2.1. Visualisation of radar data .....	9
2.2. Incorporating additional sources of information .....	11
2.3. Hyperbolas .....	11
2.4. Wide angle reflection and refraction (WARR) and Common midpoint (CMP) methods .....	12
<b>3. Use of GPR on Glaciers .....</b>	<b>14</b>
<b>4. GPR and permafrost .....</b>	<b>17</b>
<b>5. Conclusion .....</b>	<b>20</b>
<b>6. Acknowledgements .....</b>	<b>20</b>
<b>7. Literature .....</b>	<b>21</b>

## Abstract

Ground penetrating radar (GPR) provides a powerful tool for subsurface remote sensing and as several companies offer commercial units, it also becomes increasingly convenient and inexpensive to use. Since the introduction of GPR about twenty years ago much success in employing it on glaciers and on permafrost has been reported, and methods as well as equipment have been greatly improved.

After a very short introduction to some glaciological terms which are important for GPR sounding the dielectric behaviour of ice is described and explained in section 3. Different examples of glaciological work with radar from the literature are given.

In section 4, terms and properties of permafrost that are relevant to GPR remote sensing as well as dielectric behaviour of frozen ground are explained. Also, some examples of radar soundings in permafrost and their limitations, as available from literature, are presented.

The sections about GPR usage on glaciers and permafrost are preceded by a general introduction which covers relevant aspects of electromagnetic radiation and its interaction with matter as well as basic principles and physics involved in GPR remote sensing. A chapter on visualisation and interpretation of radar data completes this general introduction.

## Introduction

When we were first introduced to ground penetrating radar we found ourselves confronted with a multitude of terms and methods that we did not understand and no good introduction to this technique was available. Being fascinated by the capabilities of this method we wanted to gain some understanding in order to employ it.

The idea of this study paper is to explain processes, methods and terms needed for the application of GPR in our present main field of study: glacial and periglacial environments. We aim at a level of explanation sufficient to meaningfully use GPR but yet not to go into too much detail. After all we want to study earth and not physics.

The Equations used herein refer to SI units unless otherwise stated.

This document is available on the internet, see last page of this paper.

# 1. Understanding radar

## 1.1. Electromagnetic radiation

In order to give a better understanding of radar remote sensing it is essential to have a short introduction into the nature of electromagnetic radiation (EMR). The content of this chapter will follow Kip (1969) and Drury (1993).

EMR consists of quanta which are the smallest defined units of energy and can be described as particles (photons) or as waves of oscillating electric and magnetic fields. The explanation of radar remote sensing in this paper will deal with EMR as waves, only.

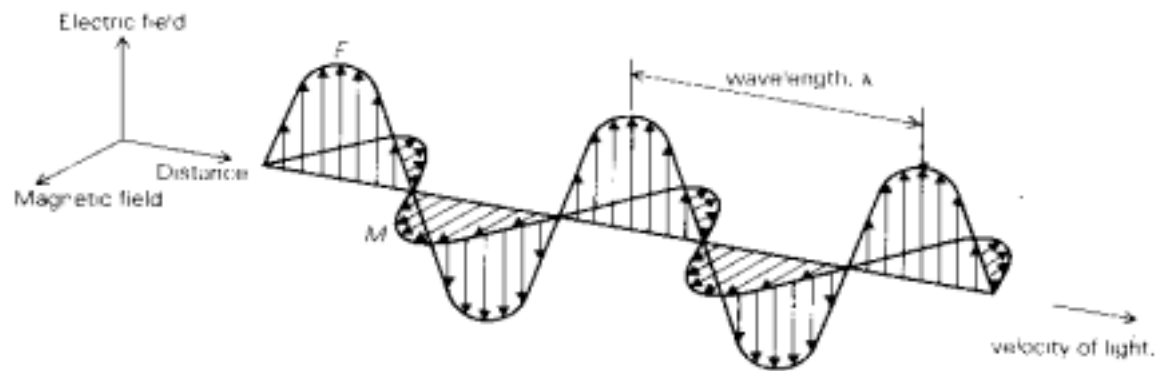


**Figure 1 Propagation of electromagnetic radiation (Drury 1993)**

These oscillating fields stand in right angles to each other and to the direction of propagation. The oscillations can be described as sine waves. If the electric fields of all quanta are lined in one direction the radiation is called polarised.

The velocity of propagation for EMR in a vacuum is  $c = 2.99 \times 10^8 \text{ ms}^{-1}$ . In matter this velocity changes as is shown later.

$$c = \frac{1}{\sqrt{\epsilon_0 \mu_0}} \quad \text{Equation 1}$$

$\epsilon_0$  and  $\mu_0$  are the free space (in vacuum) constants for permittivity and permeability. Permittivity is the property of a dielectric substance that determines the degree in which it modifies an electric field. Permeability is the property of a magnetisable substance that determines the degree in which it modifies the magnetic flux in the region occupied by it in a magnetic field.

The frequency of the wave oscillation  $f$  and the wave length  $\lambda$  are antiproportional.

$$c = \lambda f \quad \text{Equation 2}$$

Frequency and wavelength vary as a function of the energy of the quanta according to Planck's law:

$$E = fh \quad \text{Equation 3}$$

where Planck's constant  $h = 6.62 \times 10^{-34} \text{ Js}$

EMR of different wave lengths is emitted from different sources and through different processes. Also, the behaviour of EMR changes with its wavelength.

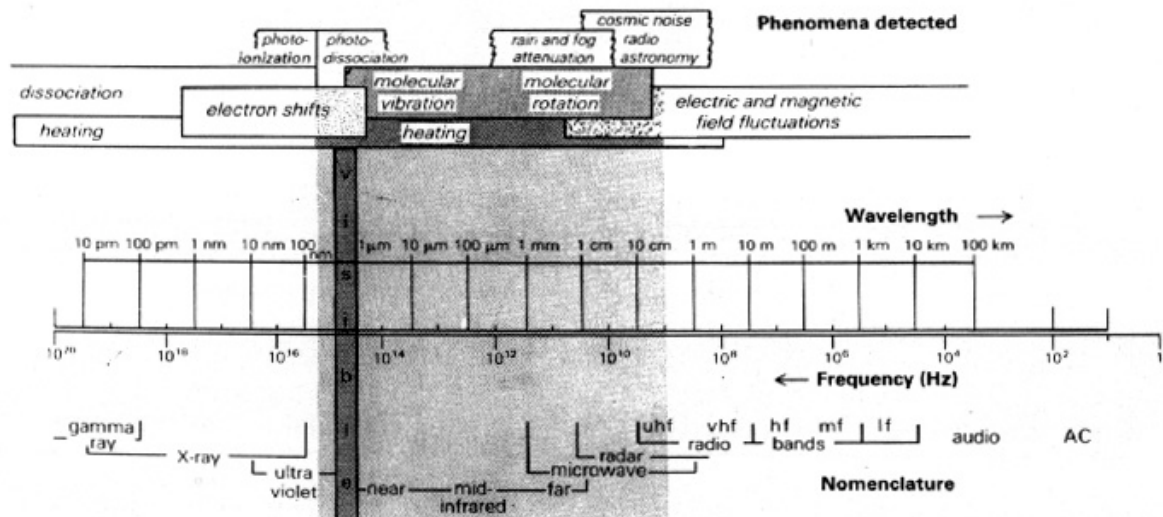


**Figure 2 Common part of the electromagnetic spectrum (Drury 1993)**

EMR is produced where size or direction of electric or magnetic fields fluctuate in time. The shortest wavelength requires the highest energy for emitting a quantum. Gamma rays, the shortest waves are a result of nuclear fission or fusion. X-rays, ultra violet and visible light are generated by electrons jumping from one stable orbiting shell to another. The energy lost by the electron jumping from a higher orbit to a lower one is thereby emitted as a quantum. Infrared and microwaves are emitted by vibration or rotation of molecules. Longer waves such as microwaves which are used in radar, and radio waves are produced by field fluctuations such as changing electrical charges in an antenna.

These different mechanisms of wave generation are also the mechanisms of interaction with matter. Therefore different materials behave differently with varying wavelengths. These changes in behaviour and velocity of EMR in a medium are the basis for radar remote sensing.

As most transparent materials are nonmagnetic they have magnetic permeabilities very close to the free space value  $\mu_0$ . Therefore the velocity in a transparent medium is in general given by its dielectric permittivity  $\epsilon$ .

Permittivity is usually expressed as the dimensionless relative permittivity  $\epsilon$  which is determined by Equation 4 where  $\epsilon_1$  is the absolute permittivity of a medium and  $\epsilon_0$  the free space constant. In this paper the term permittivity is used for relative permittivity.

$$\epsilon = \frac{\epsilon_1}{\epsilon_0} \quad \text{Equation 4}$$

Permittivity is a complex number given by:

$$\epsilon = \epsilon' + i\epsilon'' \quad \text{Equation 5}$$

Where the complex permittivity is  $\epsilon$  and  $\epsilon'$  is the so called real part of the complex permittivity which directly influences the propagation velocity of EMR in materials with no loss.  $\epsilon''$  is the imaginary part of the complex permittivity which is related to the dielectric loss of the material caused by its conductivity. Conducting materials are generally opaque for EMR. Impurities of conducting materials can change the dielectric behaviour of matter as described in chapter 3.

The velocity of EMR in a medium  $v$  is:

$$v = \frac{c}{\sqrt{\epsilon}} \quad \text{Equation 6}$$

At a boundary between media of a different permittivity, a so called dielectric boundary some of the EMR's energy is reflected and some is refracted into the other medium.

The higher the difference between the refraction indices of the two media is the more energy is reflected. With a decreasing incidence angle a bigger portion of energy is reflected, eventually leading to total reflection.

For plane waves normal to the surface the amount of energy reflected and refracted is determined by:

$$E' = \left( \frac{2n_1}{2n_2 + n_1} \right) E \quad \text{and} \quad E_1 = \left( \frac{n_2 - n_1}{n_2 + n_1} \right) E \quad \text{Equation 7}$$

where  $E$  is the amount of incoming EMR,  $E'$  is the amount of refracted EMR and  $E_1$  is the amount of reflected EMR and  $n$  is the refractive index  $n = \sqrt{\epsilon}$  of the medium.

Considering  $E$ ,  $E'$  and  $E_1$  to be the amplitude of electric field vectors no sign and therefore phase change occurs for the reflected wave  $E_1$  with  $n_1 < n_2$ . If  $n_1 > n_2$  however the sign of  $E_1$  is changed in respect to  $E$  i.e. the reflected wavelet is phase changed. Also, equation 7 demonstrates that the part of the wave that is refracted and passes through medium 2 always remains in phase.

At a dielectric boundary EMR gets either reflected, refracted in the material.

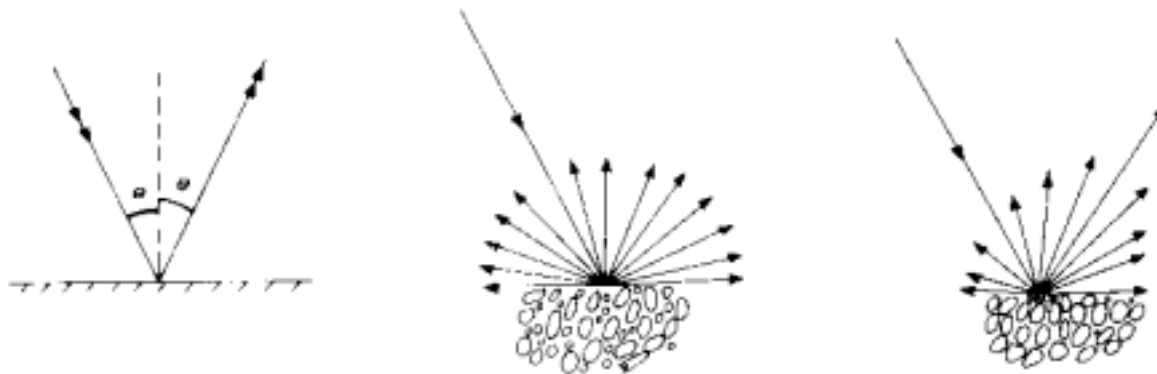


**Figure 3** Specular, diffuse and Lambertian reflections (Drury 1993)

Reflection can be specular from a smooth surface, diffuse from a rough surface or as in most cases in nature a Lambertian reflection which is the combination of both. A surface appears smooth if its texture is smaller in scale than the wavelength of the EMR reflected. If the texture is about the same scale or larger than the wavelength the surface appears rough.

## 1.2. Basic physics of radar

Only low-loss and low-conductivity materials dominated by polarisation are dealt with here, as only those are amenable for GPR sounding. (Davis & Annan 1989)

Ground penetrating radar uses EMR in the microwave range with frequencies between 10 and 1000 MHz. The interaction of those waves with matter depends on the dielectric properties of the material for the named frequencies. Generally the velocity of the radar

wave in the material varies with its dielectric permittivity. Variations in permittivity are the basis for GPR remote sensing.

The velocity in a medium  $v$  is:

$$v = \frac{c}{\sqrt{\epsilon}} \quad \text{Equation 8}$$

Attenuation increases with rising frequency, very rapidly at frequencies above 100 MHz (Davis & Annan 1989).

If radar waves meet a boundary of 2 materials with a different permittivity a part of there energy is reflected. See equation 7 in chapter 1.1.

The resolution of a radar sounding depends on its bandwidth which is the same as its frequency for a monopulse system like GPR, see chapter 1.3. Therefore wavelength limits the resolution.

Material	$\epsilon'$	$\sigma$ [mS/m]	$v$ [m/ns]	$\alpha$ [dB/m]
Air	1	0	0.30	0
Dest. Water	80	0.01	0.033	$2 \times 10^{-3}$
Fresh water	80	0.5	0.033	0.1
Sea water	80	$3 \times 10^4$	0.01	1000
Dry sand	3-5	0.01	0.15	0.01
Saturated sand	20-30	0.1-1.0	0.06	0.03-0.3
Limestone	4-8	0.5-2	0.12	0.4-1
Shales	5-15	1-100	0.09	1-100
Silts	5-30	1-100	0.07	1-100
Clays	5-40	2-1000	0.06	1-300
Granite	4-6	0.01-1	0.13	0.01-1
Ice	3-4	0.01	0.16	0.01

**Table 1** Parameters relevant to GPR of selected materials (Davis & Annan 1989)

Table 1 shows the permittivity  $\epsilon$  and the velocity  $v$  of the radar wave in the most important geologic materials. Furthermore the conductivity  $\sigma$  and attenuation  $\alpha$  are listed. It is important to note the difference in relative permittivity for water, ice and dry or wet rock or sediments where the higher value stands for dry rock or sediments. The great difference in permittivity of liquid water to the other materials makes radar an effective tool on glaciers and permafrost where it is necessary to distinguish between water and ice or to measure water content.

GPR pulses are polarised which means that all electric field vectors are oriented in one plane and all magnetic field vectors perpendicular to it. (Davis & Annan 1989)

### 1.3. Principles of GPR applications

Ground penetrating radar is one form of radio echo sounding (RES), operating at a frequency between 10 and 1000 MHz (Davis & Annan 1989) and using a monopulse as transmitted wave. GPR is a tool for relatively shallow penetration. Usually depths of only about 50 meters are examined but also depth penetrations of 1000 meters have been achieved (Arcone et al. 1995). GPR has a very good resolution compared with other RES

techniques which are used for a greater depth penetration for example to view bedrock under a thick ice sheet.

GPR units consists principally of a control unit, a transmitter and a receiver. In modern systems these are connected by opto cables. A computer is commonly used for data collection. The transmitters and the antennas of transmitter and receiver can usually be changed to operate the GPR at different frequencies.

The transmitter generates a very short high voltage pulse and transmits it into the antenna, which emits EMR of a specific frequency into the surrounding area. It transmits a mono pulse i.e. only one wavelength long which has got the shape of a small negative, a large positive and again a small negative amplitude as shown in figure 4. It transmits only one pulse every time it receives a signal from the control unit.

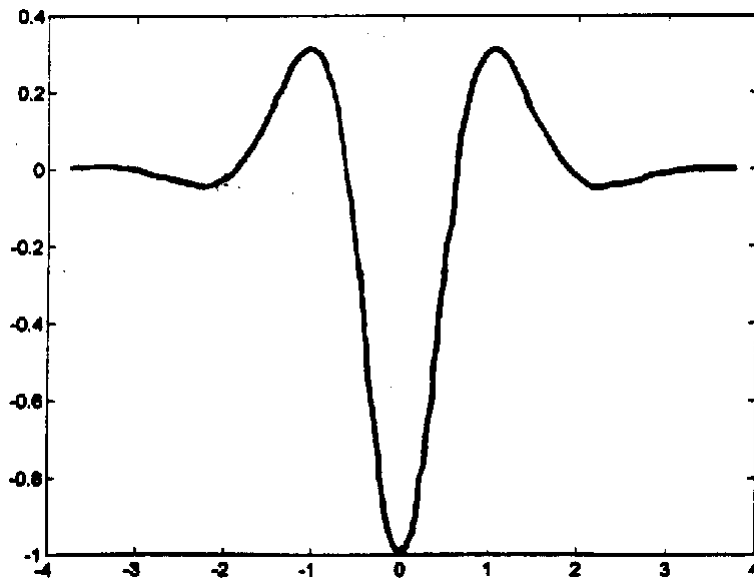


**Figure 4** Representation of a pulse transmitted by a GPR system

The receiver collects incoming signals in samples which are a digital representation of the amplitude and phase of the signal in a certain unit of time. In modern GPR units a sample is recorded as a 16 bit number. This is important for the systems resolution, especially if a weak echo from a greater depth is displayed with increased amplitude by a gain amplifier, see chapter 2.1.

To improve a systems ratio between signal and noise, several samples that have been recorded simultaneously can be put together to a so called stack by calculating their mean value.

GPR systems transmit a bandwidth of frequencies that is equal to their centre frequency, the frequency where most energy is emitted. The pulse length is inversely proportional to the centre frequency. (Davis & Annan 1989) As GPR represents a mono-pulse system (pulse of one wavelength at the centre frequency) the pulse length is  $1/f$ . Resolution and attenuation increase with increasing frequencies and therefore with increasing bandwidths as well. This is one reason to make GPR units operable at different frequencies.

Other RES systems which are used for a greater depth penetration use longer transmitted pulses and are able to penetrate up to 5 km of ice for, example.

The transmitted radar beam can be roughly described as conical. (Arcone et al. 1995). Therefore the received signal is not only received from directly beneath the antenna but also from a larger area around.



In radar sounding there is a direct coupling between the antennas of transmitter and receiver. The signal from the transmitter which propagates directly through the air to the receiver is called the air wave. The other part of the direct coupling, the ground wave, travels on the shortest way through the ground. When separating the receiver from the transmitter, the two components of the direct coupling, air and ground wave can be distinguished as they vary in travel time due to different dielectric constants of air and the ground. See chapter 2.

Usually transmitter and receiver are placed in a fixed configuration with a defined distance to each other and moved over the ground simultaneously. A hip chain or a wheel measuring the moving velocity of the equipment can be connected to the control unit to guarantee the collecting of data at equidistant positions.

## 2. GPR data interpretation

### 2.1. Visualisation of radar data

When collecting data with a GPR unit which is moved over the ground traces are collected at equidistant positions along the profile. A trace shows the received signal at a position as follows: On one axis the amplitude of the signal and at the other the time the signal needed after the first sample was collected (signal position). This means for reflected signals the time from the transmitter to reflector and from there to the receiver the so called two way travel time is recorded.

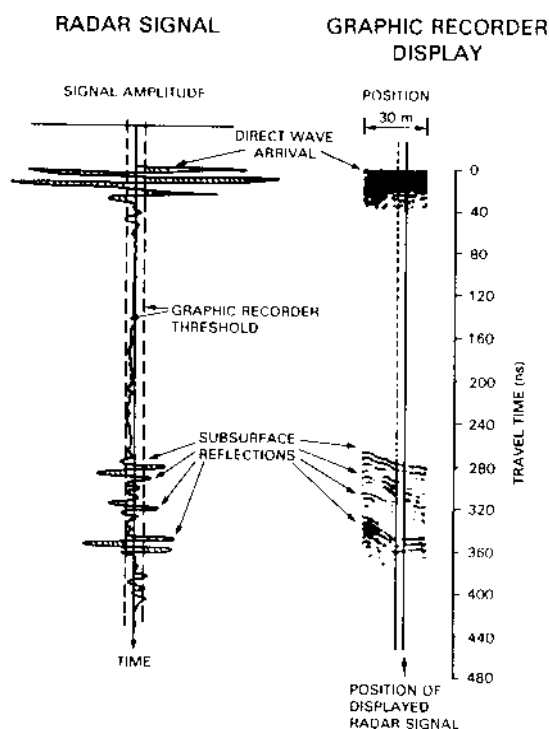


**Figure 5** A received radar signal trace accompanied by its graphic recorder display in line intensity format (Annan & Davis 1976)

As the amplitudes of the reflected signal decrease heavily with longer travel times, i.e. greater depth of the reflector, a time variable gain amplifier whose gain increases with return time is applied to the system (Annan & Davis 1976). The gain can be varied so that

it increases linear or exponential as it is required for the specific use for example at different materials or frequencies.

The single traces usually recorded will be transferred into a graphical image. The horizontal axis hereby displays the antenna position in relation to the starting point of the profile. The vertical axis represent a time scale for the radar signal delay time after signal position. If the GPR unit is not connected to an equipment measuring the right distance for collecting a trace to the previous one the horizontal axis commonly represents a time scale after the start of the profile collection (Annan & Davis 1976).

One possibility of visualisation is the so called line intensity format where single traces are not displayed and the grey level of the plot gives the amplitude of the signal for individual samples (Arcone et al. 1995), see figure 6.

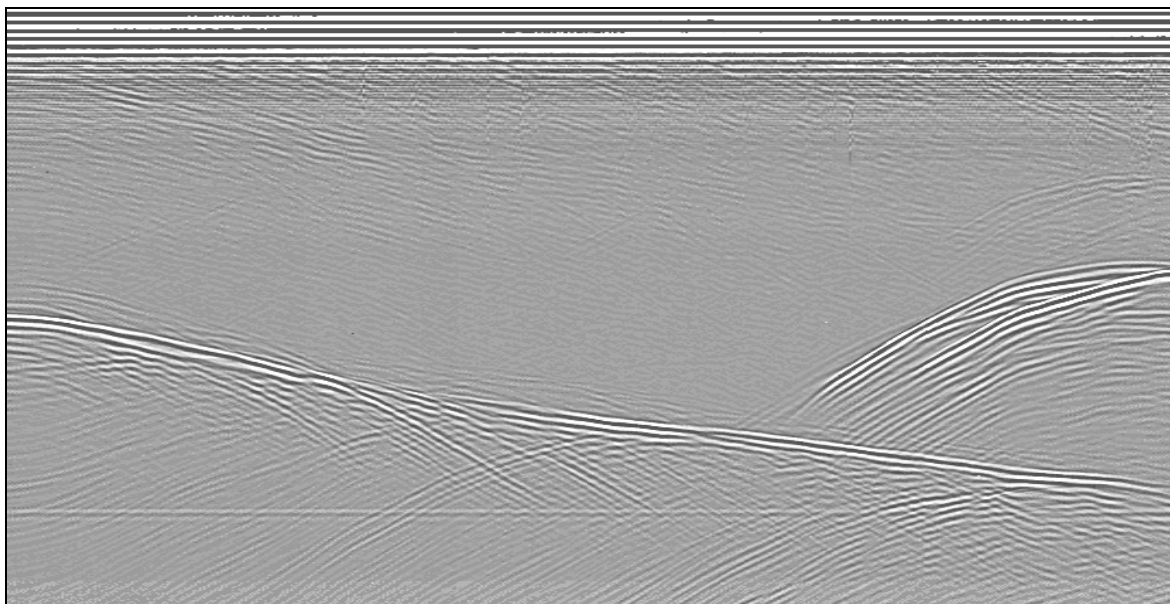


**Figure 6** Radar data displayed in line intensity format

Another way of visualisation of a recorded profile is the so-called wiggle trace image (Arcone et al. 1995) where the traces are displayed as graph of amplitude and delay time and combined to an image showing them at the position they where collected, see figure 7. Hereby the amplitudes of a strong signal recorded by neighbouring traces are overlapping each other which produces a picture similar to that given by the line intensity format.

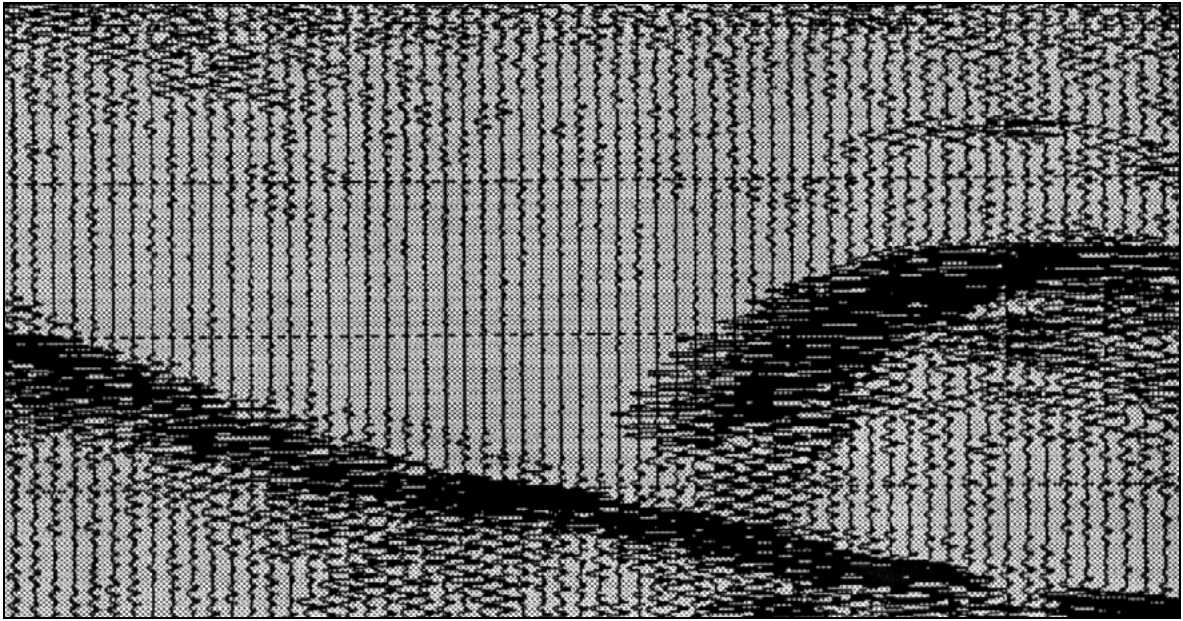


**Figure 7** Radar data displayed in wiggle trace format

## 2.2. *Incorporating additional sources of information*

The result of a GPR sounding is a qualitative statement in the form of delay time of the received signal versus signal level yielding a reconnaissance map for subsurface structures (Annan & Davis 1979). Mostly, however it is important to investigate the depth of reflectors or the properties of materials. Given the two way travel time and knowing either the dielectric behaviour of the probed terrain or the depth of reflectors the missing value can be calculated. The permittivity allows conclusions on the nature of the material it occurs in to be drawn.

The Equation below can be used for calculations in single layered systems (modified after Davis & Annan 1989).

$$d = \frac{tc}{2\sqrt{\epsilon}} \Leftrightarrow \epsilon = \left(\frac{tc}{2d}\right)^2 \Leftrightarrow t = \frac{2d\sqrt{\epsilon}}{c} \quad \text{Equation 9}$$

where  $d$  is the depth to a reflector,  $t$  is the two way travel time of the radar pulse,  $c$  is the speed of light in vacuum and  $\epsilon$  is the permittivity of the material overlying the reflector.

The depth of horizons or point reflectors can be obtained through probing, drilling and core sampling, digging or various other geophysical methods. Values of the permittivity can either be approximated from a look up table or measured on samples. In addition, two ways to determine the depth of a reflector or permittivity by means of radar sounding are presented below.

Sampling of subsurface materials as a reference however, yields much more information and a better proof of results than pure remote sensing techniques.

## 2.3. *Hyperbolas*

GPR units assume that a reflected signal comes from directly beneath the antenna. However, radar antennas always operate with more or less conical beams; in the case of most commercial units this is about  $35^\circ$  to  $45^\circ$ . This means that a return signal can be

recorded even though the antennas are not directly over a reflecting object. The radar sees this target from a number of different angles but always records it as if it was directly underneath the location of this trace which produces the characteristic hyperbolic shape (ERA 1996) as illustrated in figure 8.

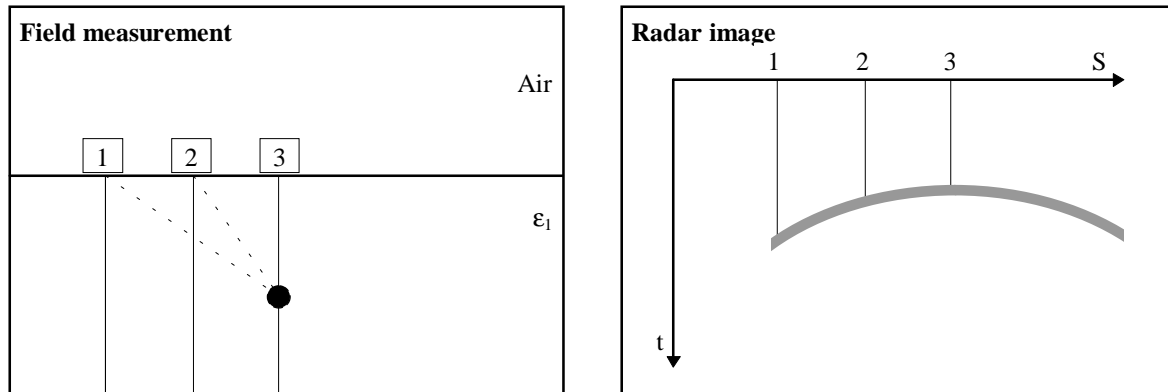


**Figure 8** Generation of hyperbolas in radar images (after ERA 1996).

The numbers 1,2 and 3 show the positions of the GPR unit in the field survey and their traces in the image that was produced. The dotted lines indicate the distance between the radar unit and the reflector. These distances are used as if they were vertical travel times in the radargram.

In the produced image the highest point of the hyperbola indicates the actual position of the reflector assuming that it is not out of the profile sideways.

Some software packages for GPR data processing include features for the calculation of the permittivity of the material overlying the reflector from hyperbolas. Also, hyperbolic shapes can be removed from radar images, i.e. the reflected signal assigned spatially to its real source, by a process called migration (Arcone et al. 1995).

#### *2.4. Wide angle reflection and refraction (WARR) and Common midpoint (CMP) methods.*

Wide angle reflection and refraction (WARR) and Common midpoint (CMP) surveys are used to obtain an estimate of the radar signal velocity versus depth in the ground by varying the antenna spacing at a fixed location and measuring two-way-travel times of the returned signals (Davis & Annan 1989).

Figure 9 shows a simplistic diagram of signal arrival in a WARR sounding over a non-inclined single subsurface interface:

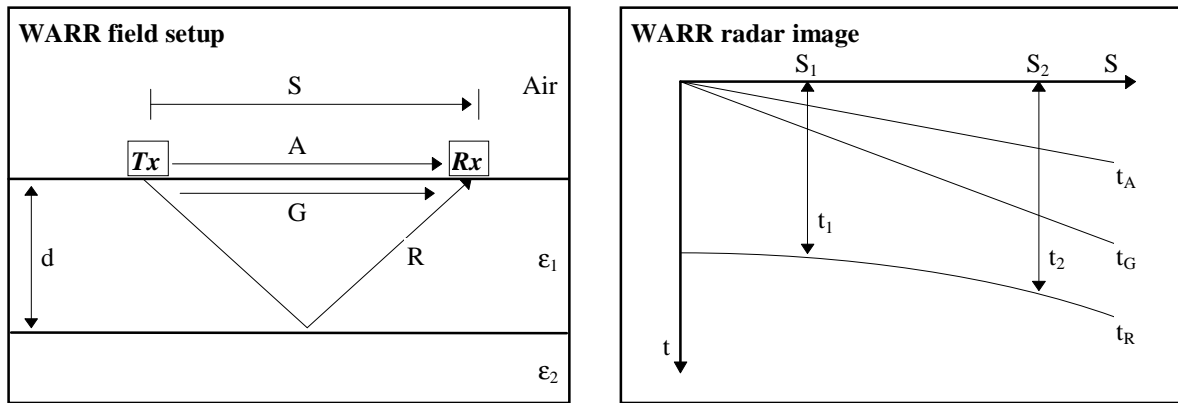


**Figure 9** Schematic representation of a WARR survey and the terms used therein (after Annan & Davis, 1976)

Air wave A, ground wave G and the reflected signal R always produce the characteristic image of two straight and one concave line. S represents antenna spacing, d the depth of the reflecting horizon and  $\epsilon_1$  and  $\epsilon_2$  refer to different permittivities of subsurface materials. Tx is the transmitter and Rx the receiver of the system. If S is not recorded it can be calculated from the arrival time of the air wave  $t_A$  and the speed of light in air c using  $S = ct_A$ .

The arrival time of the ground wave  $t_G$  and antenna separation S yield the signal velocity in the near surface ground  $v_G$  and  $t_G$  and  $t_A$  yield an approximation of the permittivity of the near subsurface:

$$v_G = \frac{S}{t_G} \quad \epsilon = \left( \frac{t_A}{t_G} \right)^2 \quad \text{Equation 10}$$

The depth d to the reflecting horizon is given by:

$$d = \sqrt{\frac{t_2^2 S_1^2 - t_1^2 S_2^2}{4(t_1^2 - t_2^2)}} \quad \text{Equation 11}$$

The permittivity above this horizon  $\epsilon_1$  can be derived by:

$$\epsilon_1 = \left( \frac{ct_0}{2d} \right)^2 \quad \text{Equation 12}$$

where  $t_0$  is the two-way-travel time with minimum antenna spacing i.e. a vertically travelling signal. Some software packages for radar data processing feature WARR-interpretation capabilities.

The common midpoint method (CMP) is a variant of WARR that is less sensitive to inclinations between surface and internal reflectors because reflection always occurs at approximately the same point as figure 10 illustrates:

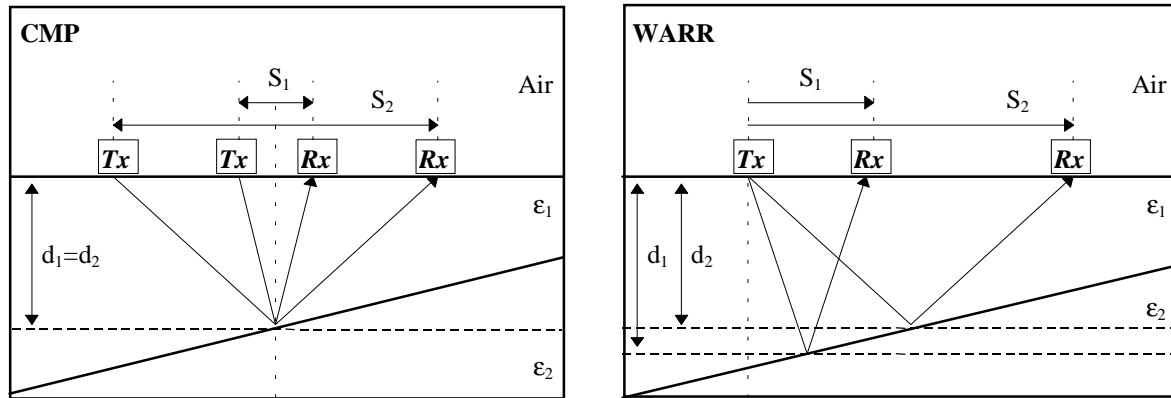


**Figure 10** On sloped reflecting horizons WARR produces a bigger error than CMP due to changing depth of the point of reflection during the survey.

In this case both, transmitter and receiver are moved apart in opposite directions at equal speed which makes CMP slower and more awkward in the field than WARR. The produced radargram as well as the data calculation are the same as for the WARR method.

Care should be taken when applying results from WARR or CMP soundings to profiles as sometimes (e.g. Judge et al. 1991) surface and subsurface conditions vary considerably over short distances.

### 3. Use of GPR on Glaciers

GPR is an efficient tool for mapping various structures on glaciers as different types of ice vary strongly in their response to radar sounding.

Glacier ice can be roughly divided into two sections: Ice which is at or close to its pressure melting point, so called temperate ice, and ice which is below this temperature, so called cold ice. Temperate ice contains various amounts of water in liquid form in cavities, channels and between grain (crystal) boundaries. Cold ice does usually not contain liquid water in channels or cavities and the amount of quasi liquid water at the grain boundaries remains less than in temperate ice and decreases with decreasing temperature.

Temperate ice is found in so called temperate glaciers and polythermal glaciers which also contain cold ice. Those glaciers are situated in mountain areas as for examples in the Alps or in subpolar regions like Svalbard. High polar glaciers and ice sheets contain usually cold ice only.

One fact that makes glaciers suitable for radar sounding is the great difference in permittivity of water in liquid and crystalline form as shown in table 1.

The difference in permittivity for water and ice at radar frequencies is due to the fact that water molecules are able to move free in the liquid while in ice they are fixed in a crystal lattice. At frequencies around 100 Hz, much lower than those used for radar the polarisation of the water molecule in the ice crystals is similar to those in liquid water and therefore permittivity of ice at those frequencies is about 90.

The frequency of radar waves still allows the water dipoles to rotate into the field direction, which is called polarisation, while the molecules in the ice crystals are now unable to rotate. This is causing the high dielectric constant of water compared to ice at radar frequencies. Therefore cold and temperate ice are usually easy to distinguish by GPR.

At higher frequencies (GHz) the field oscillations are too fast to allow the dipoles to rotate and the dielectric constant of liquid water becomes similar to what the one of ice is at radar frequencies. (Moore1988)

Furthermore the density of the ice or firm meaning the ratio between ice and air causes changes in permittivity and therefore velocity of the radar waves as expressed by Robin in his equation which is only valid for dry ice or firm: (Kohler et al., in press)

$$D = \frac{ct}{2(1+0.85\rho)} \quad \text{Equation 13a}$$

$$\sqrt{\varepsilon_d} = 1 + 0.00085\rho_d \quad \text{Equation 13b}$$

where D is the depth to the reflecting horizon, t is the two way travel time to the reflecting horizon and  $\rho$  is the average density of the firm or ice above the reflecting horizon in  $\text{kg m}^3$ .  $\varepsilon_d$  and  $\rho_d$  are the permittivity and the density of dry ice or firm.

The permittivity can be calculated after equation 13b for its relation to the density of dry ice for firm denser than  $300 \text{ kg/m}^3$ .

Equation 14 and 15 show a quantitative relation between permittivity and water content in temperate ice.

To calculate the difference in permittivity of dry and wet ice or firm due to large concentrations of spherical air or water inclusions with known water content by volume the equations by Looyenga (1965, quoted in Macheret et al. 1993) can be used:

$$\sqrt[3]{\varepsilon_d} = 1 + \theta(\sqrt[3]{\varepsilon_i} - 1) \quad \text{Equation 14}$$

$$\sqrt[3]{\varepsilon_s} = \sqrt[3]{\varepsilon_d}(1 - \theta)(\sqrt[3]{\varepsilon_w} - \sqrt[3]{\varepsilon_d}) \quad \text{Equation 15}$$

where  $\varepsilon_d$  is the permittivity of dry ice or firm,  $\varepsilon_s$  is wet ice or firm  $\varepsilon_i$  is dry solid ice with a known permittivity of 3.2,  $\varepsilon_w$  is the permittivity of water, and  $\theta$  is water content expressed as a percentage. A good approximation of the permittivity for dry ice or firm above  $300 \text{ Kg}$  per cubic meter is already given by equation 13b.

If water inclusions are distributed randomly throughout the ice, Pears equation (Macheret et al. 1993) can be used as shown in equation 16:

$$\varepsilon_s = \varepsilon_d + \frac{1}{3}(1 - \theta)\varepsilon_w \quad \text{Equation 16}$$

Where  $\varepsilon_d$  could be taken from equation 13b.

If velocity, or the permittivity, is known for example from a WARR survey those equations can be used to estimate the water content.

Internal reflectors corresponding to layers of different permittivity due to water content are often found in polythermal glaciers. These glaciers contain a cold upper layer and a temperate, water saturated lower layer with a high permittivity in their middle section. Those boundaries usually form a reflection horizon for radar waves.

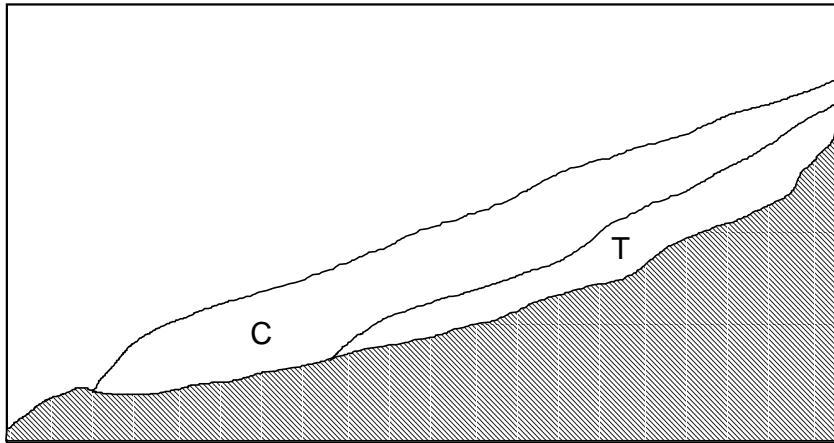


**Figure 11 Schematic profile of a polythermal glacier. C is cold ice, T is temperate ice and shaded area is bedrock. The transition, which is a line here, would appear as a reflecting horizon on a radar profile.**

Temperate ice sometimes shows different reflection areas due to layers of changing water content in cavities or channels such as the two temperate layers in Hansbreen mapped by Macheret (Macheret et al. 1993)

The best time to use GPR on glaciers in temperate regions is winter or spring to avoid a wet ice surface layer with high thaw water content which would decrease the penetration depth. (Macharet et al. 1993)

GPR has been used on polythermal glaciers for mapping internal structures, i.e. cold and temperate ice layers, but also for detecting smaller structures like crevasses and large water and air filled cavities. For detection of the structures permittivity relative to the overlying, the phase change of the reflected radar wave can be viewed (Arcone et al. 1995).

In general radar waves of higher frequencies are commonly used to detect internal structures of glaciers due to their higher resolution while lower frequencies are more suitable to penetrate the ice to view the bottom topography. (Bjoernson et al. 1996) Those lower frequencies are more commonly used by other RES techniques.

Impurities such as silt and debris cause a higher permittivity due to slightly higher permittivities of rock material to dry ice and to the scattering effects due to the reflections on the particle surface (depending on size and wavelength). Such impurities help detecting layers of basal ice (Arcone et al. 1995).

GPR has been used at high frequencies (500 MHz) for mass balance measurements on temperate glaciers to detect the last summers surface under the winter snow at the end of the winter season (Kohler et al. in press). In ablation areas and superimposed ice the reflection of the ice layer was used while in the accumulation area the ice layer is thin and density changes can be detected. The amount of snow could be calculated by Robins Equation when knowing the density or depth. To proof the method and to get additional data about the depth of the layer, cores were drilled and dielectric measurements were taken in combination to manual sounding and visual stratigraphy.

Radar has been used to map older annual layers in glaciers. Those are thought to reflect radar waves due to density changes and changes in crystal structure.

As the resolution of the radar depends on its frequency it is possible to use a multi frequency radar to detect the size of a point reflector by finding the boundary frequency



that just detects it. This method was used to scale crevasses and bottom structures in Antarctic ice streams.

Another factor that causes reflection in ice is the change in conductivity due to chemical impurities, which are mainly situated at grain boundaries. This becomes important in polar ice sheets where changes in conductivity are more thought to cause internal reflections than permittivity changes in a depth greater than a few hundred meters. Therefore this soundings are more commonly done by other RES techniques due to the required depth of penetration. As high polar ice sheets contain generally cold ice only the internal reflections are not caused by changes in permittivity which is shown to be mainly a function of depth due to increasing density, see equation 13b. The reflections are caused by different conductivities which are due to changes in acidity and other chemical impurities due to volcanic eruptions and changes in climatic conditions. The ice of the Greenland ice sheet for example that was deposited during the Wisconsin glaciation period is alkaline due to higher amounts of dust while the Holocene is acidic. Those conductivity changes are much greater than those found by density changes (Moore 1988).

## 4. GPR and permafrost

Permafrost is defined as any material that maintains a temperature below 0 °C for at least two years. For practical reasons however it is widely accepted to use the term permafrost where temperatures remain below 0 °C over one summer.

Especially in areas without continuous permafrost its occurrence and properties show a strong lateral variability in response to exposition, ground composition local hydrology and microclimate. Permafrost is also subject to temporal variations in response to changes in surface conditions or climate and therefore of interest for investigations of global warming trends.

The practical interest in investigating permafrost arises from the continuing expansion of infrastructure into areas with permafrost occurrence. As geologic materials exhibit very different physical behaviours in the presence of liquid water or ice it is vital basis for planning and engineering to know the spatial and temporal variations in freezing and thawing of the ground that underlies and surrounds a planned object. Furthermore it can be desirable to monitor the formation or degradation of permafrost due to human activities and there is a scientific interest in investigating permafrost distribution and properties.

As the application of GPR on permafrost uses the strong dielectric contrast between liquid water and ice to distinguish between frozen and unfrozen materials it is not suitable for detecting dry permafrost i.e. frozen bedrock. GPR responds to the physical properties of the ground and does not reveal the actual composition of soil or rock (Judge et al. 1991). Therefore additional information e.g. from bore holes is needed if the exact composition of subsurface materials is of interest. In most cases however investigating permafrost primarily means the detection of interfaces between materials containing liquid and frozen water. Additionally the exploration of stratigraphy and of massive ground ice are often desirable.

As figure 13 shows, most frost interfaces exhibit annual variations. Some shallow diurnal fluctuations can be observed, too. It is therefore necessary to carefully consider the timing of a GPR survey on permafrost depending on the aim of it.

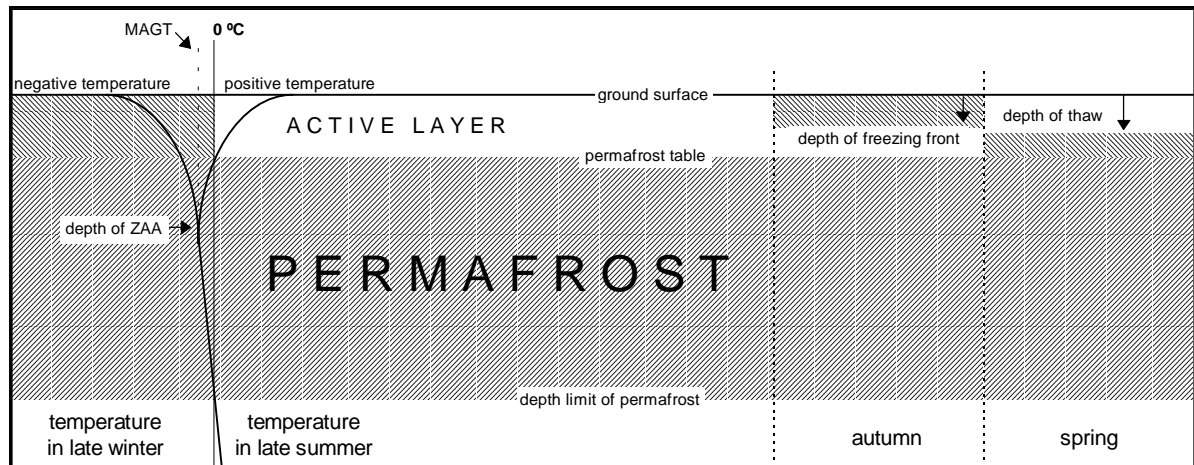


**Figure 12 Schematic cross-section of permafrost (after King, 1984)**

Figure 12 shows a vertical section through ground containing permafrost in order to define some frequently used terms. The ground temperature regime is shown schematically for late winter and late summer, and the mean annual ground temperature (MAGT) as well as the depth of the zero annual amplitude (ZAA) are indicated. As ice wedges, which are not shown in this diagram, do not extend into the active layer (Williams & Smith 1989) their detection can give an estimate of the depth of the permafrost table.

The depth to which a radar pulse will effectively penetrate is dependent upon the power and performance of the system, the frequency of the pulse, the number and strength of reflecting interfaces and the attenuation properties of subsurface materials.

GPR produces better results in well-drained, coarse materials than in fine grained ones as granular material produces less signal attenuation (Judge et al. 1991). In sand, gravel and rock GPR has been demonstrated to sound to depths of 50 m but the range decreases to a few meters in conductive materials such as moist silts or soils with saline pore water (Davis & Annan 1989). Clays are virtually opaque to microwaves. Also, the presence of boulders and blocks larger than one wavelength attenuates the signal due to scattering and thus reduces the depth of sounding.

The electric/dielectric properties of ground materials are partly determined by their dry characteristics i.e. grain size distribution, porosity and mineral composition. In dependence on these dry properties the amount of liquid water, ice and air present in the ground greatly influences its electric/dielectric properties and thus reflection from interfaces and attenuation of the transmitted signal.

Pore water usually freezes and therefore effects a significant change in the ground dielectric constant at 0 °C. Fine grained materials however, have the ability to retain a some molecules thick layer of unfrozen water even several degrees below zero as shown in figure 14. Between 0 and -1.5 °C capillarity is responsible for much of the freezing point depression (Williams & Smith 1989). The amount of water adsorbed on particle surfaces or kept liquid in capillaries is a function of the particle surface, i.e. grain size distribution, and its temperature.

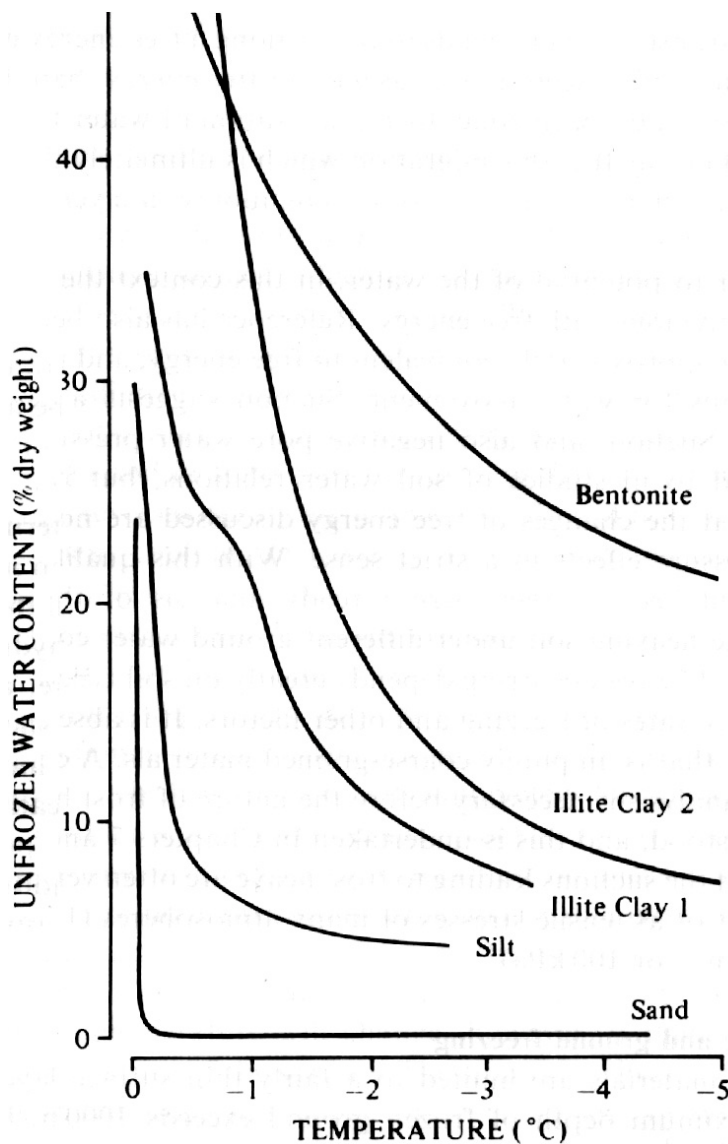


**Figure 14** Amount of unfrozen water at different temperatures for various soils. (Williams & Smith 1989)

A very high permittivity due to rotation of molecules and due to ionic charge carriers (Moore 1992) in this liquid water can be observed below freezing. Mobile charge carriers also increase the conductivity and therefore the signal attenuation in a material.

To illustrate the resulting dielectric behaviour of ground materials we consider a dry, fine grained matrix with a permittivity lower than ice and a certain porosity. Increasing the water content of this material from 0 to 100 % will result in a non-linear response of permittivity (Arcone & Delaney 1989) at natural temperatures below zero: Having no water content the permittivity will be given by the value for the material itself and for the air contained in the pores at any temperature. Increasing the water content, a state will be reached where all water is adsorbed on soil particles at a given temperature below zero and the remaining pore volume is occupied by air. Until that point is reached a rapid increase of the permittivity can be observed as all water remains liquid in adsorption. After the point of full adsorption, the remaining air in the pores is gradually replaced by pore ice thus slowly increasing the permittivity until saturation is reached. Further increasing the water and therefore ice content after saturation will subsequently lower the permittivity (Arcone & Delaney 1989) to that of ice at 100 % ice content, finally.

Similarly for massive ground ice dielectric behaviour can change in dependence on the amount of air trapped in it and on the amount and type of impurities contained in it. Furthermore temperature which affects the amount of liquid water in it determines its permittivity.

For these reasons the use of radar alone to predict the ice content of soil (Annan & Davis 1976) or the amount of air in massive ground ice is not feasible as too many variables are involved in determining ground dielectric properties.

Ground penetrating radar has been successfully used in detecting ground ice bodies and in mapping the seasonal depth of thaw in permafrost areas (e.g. Judge et al. 1991). Where within its depth penetration range it may also be employed to detect the lower limit of frozen material in the ground, preferably in spring when the active layer is completely frozen. In areas with discontinuous permafrost ground penetrating radar can be used to detect isolated bodies of frozen ground. GPR is able to fairly precisely define stratigraphic units two-dimensionally which could be extended towards three-dimensional profiles (e.g. Judge et al. 1991). For the detection of the mostly very distinct interfaces between thawed and frozen ground GPR may be employed without the aid of other geophysical methods. Borehole information or other additional sources of information are needed however to refer the exact composition of the detected ground materials like air content in massive ice or ice content in soil.

## 5. Conclusion

Ground penetrating radar is a capable instrument for mapping various structures on glaciers as well as for investigating permafrost. However, in many cases further information from different sources is required to interpret the radar data. Especially on permafrost GPR surveys strongly depend on additional data from e.g. bore holes or seismic measurements as ground dielectric properties have a very complex dependency on different material compositions and on temperature and are therefore hard to interpret. On glaciers reflections are easier to interpret as their causes are more limited. WARR or CMP surveys can provide quantitative information to make GPR soundings more independent from additional data collected by other techniques.

## 6. Acknowledgements

This study paper and our interest in GPR has been supported by our supervisor Dr. John Moore with much commitment and patience. Neil Parry of EBA Engineering Consultants Ltd., Edmonton, Canada, Brian Mooreman from the University of Calgary, Canada and Pekka Majala from the University of Oulu, Finland pointed out sources of information to us and answered some specific questions. Furthermore, ERA Technology, Surrey, England and Toikka Oy, Espoo, Finland, kindly supplied information on their commercial radar units. Prof. Lorenz King from the University of Gießen made some of his work about geoelectrical and seismic permafrost detection available to us.

We thank all these persons and institutions.

Alison Tracey made the drawing on the cover-page. Thanks a lot.

## 7. Literature

- Acorne, S.A. and Delaney, A.J. 1984.** Field dielectric measurements of frozen silt using VHF pulses. *Cold Regions Science and Technology* 9, 1984. pp. 29-37.
- Acorne, S.A. and Delaney, A.J. 1989.** Investigations of dielectric properties of some frozen materials using cross-borehole radiowave pulse transmissions. CRREL Report 89 (4), 1989.
- Acorne, S.A., Lawson, D.E. and Delaney, A.J. 1995.** Short-pulse radar wavelet recovery and resolution of dielectric contrasts within englacial and basal ice of Matanuska Glacier, Alaska, U.S.A. *Journal of Glaciology* 41 (137), 1995. pp. 68-86.
- Annan, A.P. and Davis, J.L. 1976.** Impulse radar sounding in permafrost. *Radio Science* 11, 1976. pp. 383-394.
- Bjoernson, H., Gjesing, Y., Hansen, S., Hagen, J.O., Padsson, F., Erlingsson, B. 1996** The thermal regime of sub polar glaciers mapped by multi frequency radio echo sounding. *Journal of Glaciology* 42 (140), 1996.
- Davis, J.L. and Annan, A.P. 1989.** Ground-penetrating radar for high resolution mapping of soil and rock stratigraphy. *Geophysical Prospecting* 37, 1989. pp. 531-551.
- Drury, S.A. 1993.** Image interpretation in geology. pp. 1-4, 41-47, 175-203. Chapman & Hall, London, 1993.
- ERA Technology (1996),** SPRscan - producing results. EBA Technology, Surrey KT22 7SA, England.
- Hall, D.K. 1985.** Remote sensing of ice and snow. pp. 1-22, 109-155. Chapman & Hall, London, 1985.
- Judge, A.S., Tucker, C.M., Pilon, J.A. and Moorman, B.J. 1991.** Remote Sensing of Permafrost by Ground-Penetrating Radar at Two Airports in Arctic Canada. *Arctic* 44 Supplement 1, pp. 40-48.
- King, L. 1984.** Permafrost in Skandinavien. Untersuchungsergebnisse aus Lappland, Jotunheimen und Dovre/Rondane. Dept. of Geography, University of Heidelberg, Heidelberger Geographische Arbeiten, 76.
- Kip, A.F., 1969.** Fundamentals of Electricity and Magnetism. International student edition. McGraw-Hill Kogakusha Ltd, Tokyo.
- Kohler, J., Moore, J., Kennt, M., Engeset, R., Elvehoey, H. 1997, in press.** Using ground penetrating radar to find last year's summer surface in mass balance measurements: what are we really seeing ?
- Macharet, Y.Y., Moskalevsky, M.Y., Vasilenko, E.V. 1993.** Velocity of radio waves in glaciers as indicator of their hydrothermal state, structure and regime. *Journal of Glaciology* 39 (132), 1993.
- Maeno, N., Araki, T., Moore, J. and Fukuda, M. 1992.** Dielectric Response of Water and Ice in Frozen Soils. In: Maeno, N. & Hondoh, T. (ed). *Physics and Chemistry of Ice*. Hokkaido University Press. 1992, Sapporo.
- Malå GeoScience 1995.** RAMAC-GPR - Operating Manual. Malå GeoScience, Skolgatan 11, 93070 Malå, Sweden.

**Moore, J.C., 1988a.** Dielectric variability of a 130 m Antarctic ice core: Implications for radar sounding. *Annals of Glaciology* 11. 1988.

**Moore, J.C., 1988b.** Geophysical aspects of ice core drilling in Antarctica., Ph. D. British Antarctic Survey. Cambridge, England.

**Telford, W.M., Geldart, L.P. and Sheriff, R.E. 1990.** Applied Geophysics - Second Edition. Cambridge University Press, Cambridge 1990.

**Williams, P.J. and Smith, M.W. 1989.** The frozen earth. Cambridge University Press, Cambridge 1989.

This document is available on the internet. It can be viewed in HTML or downloaded in pdf format, including all graphics.

**<http://www.sgruber.de/pap-rad.htm>**

**Stephan Gruber / Florian Ludwig**  
c/o Geographisches Institut/JLU Gießen  
Senckenbergstraße 1  
35390 Gießen, Germany  
email: mail@sgruber.de

**Dr. John Moore**  
Arctic Centre  
Box 122  
96101 Rovaniemi, Finland  
email: jmoore@levi.urova.fi  
Ph. +358 16 324 757  
Fax: +358 16 324 777